Supporting Online Materials for

EZH2 Oncogenic Activity in Castration Resistant Prostate Cancer is Polycomb-Independent

Kexin Xu, Zhenhua Jeremy Wu, Anna C. Groner, Housheng Hansen He, Changmeng Cai, Rosina T. Lis, Xiaoqiu Wu, Edward C. Stack, Massimo Loda, Tao Liu, Han Xu, Laura Cato, James E. Thornton, Richard I. Gregory, Colm Morrissey, Robert L. Vessella, Rodolfo Montironi, Cristina Magi-Galluzzi, Philip W. Kantoff, Steven P. Balk, X. Shirley Liu*, and Myles Brown*

*To whom correspondence should be addressed. E-mails: xsliu@jimmy.harvard.edu (X.S.L.), myles_brown@dfci.harvard.edu (M.B.)

This PDF file includes:

Materials and Methods

Prostate cancer cell culture. All prostate cancer cell lines were propagated as previously described (*23, 24*). LNCaP cell line was obtained from the American Type Culture Collection. LNCaP-abl (abl) cell line was kindly provided by Zoran Culig (Innsbruck Medical University, Austria). C4-2B cell line was obtained from ViroMed Laboratories (Minneapolis, MN). CWR22Rv1 cell line was generously provided by Dr. Steven Balk (Beth Israel Deaconess Medical Center, MA).

Plasmids and reagents. Plasmids for Myc-tagged, siRNA-resistant (SR) wild-type EZH2 (E^{sr}-WT) was kindly provided by Dr. Haojie Huang (Stony Brook University Medical Center, NY), which contains synonymous base substitutions that render it resistant to the siRNA-mediated silencing. Amino-acid substitution mutants of EZH2 [E^{sr}-DM ($EZH2^{H694A/F672I}$), E^{sr}-S21A, E^{sr}-S21D, E^{sr}-T350A (T345 in mouse Ezh2) and E^{sr}-T492A (T487 in mouse Ezh2)] and the SET domain truncation (E^{sr}-ΔSET) were generated using QuikChange II XL site-directed mutagenesis kit with the following primers:
H694A, 5'-GGTAACAAAATTCGTTTTGCAAATGCTTCGGTAAATCCAAACTGCTATGC-3'; F672I, 5'-GCAGCTTTCTGATCAACTTGAAC-3'; ΔSET, 5'-CAGTATTCAGCGGGGCTCCTAAAAGCATCTATTGCTGGC-3'; S21A, 5'-GGCGGAAGCGTGTAAAAGCAGAGTACATGCGACTGAG-3'; S21D, 5'-GGGACCAGTTTGTTGGCGGAAGCGTGTAAAAGACGAGTACATGCGACTGAGACAGC TCAAGAGG-3'; T350A, 5'-GCTGAGCGGATAAAGGCCCCACCAAAACGTCCAG-3'; and T492A, 5'-CCCGCTGAGGATGTGGATGCTCCTCCAAGGAAAAAGAAG-3'. Plasmids expressing EZH2 deletion mutants were generously provided by Dr. Yongfeng Shang (Tianjin Medical University, Tianjin, China), which are all FLAG-tagged. Constructs for untagged wild-type EZH2 and the SET domain deletion mutant were kindly provided by Dr. Arul Chinnaiyan (Michigan Center for Translational Pathology, MI). Specific antibodies used in our work include: anti-AR (sc-816), anti-c-Myc (sc-40), normal rabbit IgG (sc-2027), anti-RNA polymerase II [(sc-9001) and (sc-56767)], and anti-GAPDH (sc-32233) from Santa Cruz Biotechnology, anti-EZH2 (39639) from Active Motif and (612666) from BD Biosciences, anti-PHLPP1 (A300-660A) and anti-phospho-EZH2 (S21) (A300-529A) from Bethyl Laboratories, anti-phospho-EZH2 (T487) (3368-1) from Epitomics, anti-phospho-AKT (S473) (9271) and anti-SUZ12 (3737) from Cell Signaling Technology, anti-H3K4me2 (07-030), anti-H3K27me3 (07-449) and anti-EED (05-1320) from Millipore, anti-pan-AKT (ab8805), anti-calnexin (ab10286), anti-CKS2 (ab54644), anti-EZH1 (ab13665), anti-H3 (ab1791), anti-H3K4me3 (ab8580) and anti-RAD51C (ab55728) from Abcam, anti-AR (554224) from BD Pharmingen, anti-KIAA0101 (SAB1406878) and anti-TMEM48 (SAB2105661) from Sigma Aldrich Technology Polyclonal antibodies against the phosphorylated EZH2 at the T350 residue were generously provided by Dr. Haojie Huang (Stony Brook University Medical Center, NY) and Dr. Danny Reinberg (New York University School of Medicine, NY).

RNA interference. A control siRNA (siCtrl) and siRNAs targeting AR, EZH2 or SUZ12 were purchased from Dharmacon (Dharmacon, Lafayette, CO). siRNA targeting EED (sc-37823) was purchased from Santa Cruz Biotechnology. Lentiviral shRNA constructs for EZH2 were prepared as described before (*25*). The target sequences were listed in Table S2.

Gene expression experiments and analyses. Hormone-depleted LNCaP and abl cells were transfected with either control siRNA (siCtrl) or siRNAs targeting EZH2 (siEZH2), and LNCaP

cells were then treated with 10 nM DHT for 24 hrs, while abl cells with vehicle only. Forty-eight hours after siRNA transfection, total RNA was isolated and hybridized to Affymetrix human U133 plus 2.0 expression array (Affymetrix, Santa Clara, CA). The expression raw data for AR-dependent genes in LNCaP and abl cells were from our previous work (GSE11428) (*24*). 'Combat' is used to remove batch effects (*26*). Raw data is preprocessed using RMA with quantile normalization (*27*). Limma is applied for differential expressed gene calling (*28*). *P* value for significance cutoff is based on value after Benjamini-Hochberg multiple testing correction. Redefined custom CDF files for corresponding array platform are used in all RMA preprocessing of array data (*29*). Two independent sets of gene expression data were retrieved to check the clinic relevance of EZH2-regulated genes: Varambally (GSE3325) and Yu (GSE6919). These clinical expression data were preprocessed with the same procedure of RMA as described above.

Standard ChIP assays and ChIP-seq. Chromatin immunoprecipitation (ChIP) was performed as previously described (*30*). Briefly, 5-10X10^6 cells were cross-linked with 1% formaldehyde at room temperature for 10 min. Chromatin was sonicated to 300-500 bp in RIPA buffer with 0.3 M NaCl. 5-10 ug antibodies were incubated with Dynabead Protein A/G (Invitrogen) for at least 3 hrs before incubating with sonicated chromatin overnight. After RNase A and Proteinase K treatment, ChIP DNA was quantified by Quant-iT^{TM} dsDNA HS assay kit (Invitrogen). For targeted ChIP, extracted DNA was used for quantitative PCR (qPCR) with the specific primers as listed in Table S3. For ChIP-seq, 15-20 ng ChIP or input DNA was ligated to specific annealed linkers followed by direct sequencing using the Illumina HiSeq 2000 system at Dana-Farber Cancer Institute. ChIP-chip data sets of AR were from our previous work (*24, 31*). AR peaks of ChIP-chip data is called by MAT with FDR 5%. ChIP-seq raw data is mapped by Eland with default parameters. Each library after mapping is sampled down to 10 million reads. Only one tag from each unique position was considered to avoid PCR biases from the sequencing. The identification of ChIP-seq peaks (bound regions and summit) was performed using version 2.0 of MACS (*32*). Regions of enrichment comparing to input control exceeding a given threshold ($p <$ 1e-5) were called as peaks.

Pipeline for EZH2 peak classification. For each EZH2 enriched peak, mean wig signals of EZH2 and H3K27me3 within 4kb around the peak summit are obtained using bigwig tools from UCSC, defined as $\boldsymbol{w}_{\mathbf{ezh2}}$ and $\boldsymbol{w}_{\mathbf{k27}}$ respectively. Binomial test is used to detect significantly differential enrichment between EZH2 and H3K27me3 considering sequencing depth (10 million after sampling down). EZH2 peaks with significantly higher enrichment than H3K27me3 are identified using *p* value cutoff 0.05. This set of peaks is defined as S1. Remove any peaks from S1 that overlap with H3K27me3 peaks called by MACS and defined as S2. Further filtering out peaks with $\boldsymbol{w}_{\mathbf{k27}} > 10$ from S2 obtains the final list of solo peaks. These peaks with $\boldsymbol{w}_{\mathbf{k27}} > 10$ are outliers in S2 based on distribution of $\boldsymbol{w}_{\mathbf{k27}}$, which potentially are the regions with certain level of H3K27me3 enrichment but not significant enough to be called peaks. Ensemble peaks are the rest of EZH2 peaks other than solo peaks. This pipeline of identifying solo and ensemble peaks are applied to both LNCaP and abl ChIP-seq data.

Real-time RT-PCR. Real-time RT-PCR was performed as described before (*33*). Data are presented as mean ± standard deviation (SD). Primers used for RT-PCR are listed in Table S4.

Immunoprecipitation and immunoblot. The endogenous protein immunoprecipitations were carried out using either nuclear extracts or whole cell lysates as described previously (*33, 34*),

and then processed for western blotting as described before (*33*). The antibody used for immunoprecipitation was anti-AR (N-20, Santa Cruz Biotechnology) and anti-EZH2 (07-689, Millipore), or normal mouse IgG (sc-2025, Santa Cruz Biotechnology) and anti-EZH2 (612666, BD Biosciences).

Gel filtration chromatography. Nuclear extracts were prepared from prostate cancer cells and subjected to gel filtration chromatography as described previously (*30*). Fractions were resolved on SDS-PAGE and processed for Western blot analysis.

Cell proliferation assays. The prostate cancer cells were plated in 24-well plates (4-5x10^4 cells/well) and kept under indicated conditions. At indicated time point, the cells were trypsinized and collected. The number of viable cells was determined by Trypan blue exclusion and directly counted using a hemocytometer. Data represent means ± SD from three independent replicates. *P*-values were calculated using unpaired Student's *t*-test.

***In vivo* tumor growth in xenograft model.** Five six-week-old castrated male ICR/*scid* mice (Taconic) were used for xenograft studies. All procedures involving animal protocols were approved by IACUC at Beth Israel Deaconess Medical Center. Approximately 2X10^6 viable CWR22Rv1 cells expressing EZH2 shRNA were resuspended in 1ml 50% growth factor-reduced Matrigel (BD Biosciences) and injected subcutaneously into one flank of each mouse, and the same number of cells expressing scrambled control shRNA in the opposite flank. The xenografts tumor volume was determined by direct measuring three dimensions of the tumors and calculated using the formula: length X width X height. Growth curves were plotted as mean tumor sizes ± standard error of the mean (SEM) (n= 5 mice/group). *P*-values were calculated using unpaired Student's *t*-test.

Immunohistochemistry (IHC). Tumor specimens from two separate cohorts were employed for IHC analysis. In the first cohort, 82 neoadjuvant organ-confined prostate cancer cases were included on three tissue microarrays (TMAs), while the second cohort included multiple metastatic lesions from 23 CRPC cases distributed over three TMAs. All TMAs were analyzed for EZH2, pEZH2 (S21), and H3K27me3 expression using brightfield image analysis coupled with CRi image spectroscopy. Briefly, 5µm formalin-fixed, paraffin-embedded (FFPE) TMAs were deparaffinized in xylene, followed by a graded alcohol rehydration. Antigen retrieval was performed by microwaving tissues in citrate buffer [for pEZH2(S21) and H3K27me3] or EDTA buffer (EZH2) for 5 min, 3 separated times. Primary antibody incubation with EZH2 antisera (1:50; Novacastra, Leica, Butler Grove, Il), pEZH2 antisera (1:100; Abcam, Cambridge, MA), or H3K27me3 (1:200; clone C36B11, Cell Signaling Technology, Billerica, MA) was performed for 1 hour at room temperature using a BioGenex i6000 automated staining platform (BioGenex Laboratories Inc., Fremont CA). Detection of each primary antibody was carried out using Dako EnVision+ System Polymer-HRP secondary anti-rabbit or anti-mouse antibodies (Dako, Carpinteria, CA). Visualization of each target was accomplished using the EnVision+ 3-amino-9-ethylcarbazole (AEC) chromogen. The TMAs were subsequently counterstained with hematoxylin, and dehydrated in a graded series of alcohol prior to coverslip application. Slides were scanned using a Vectra multispectral imaging system (Caliper Life Sciences, Hopkinton, MA), attached to a Leitz Diaplan fluorescence microscope. After image acquisition, analysis was performed using the Caliper InForm software to identify all prostate tumor within each sample TMA core. With tumor identification confirmed by pathologists (ML and RTL), the AEC and hematoxylin spectra were unmixed, and the resulting AEC intensity (optical density, OD) for

each cell of the tumor, within both the cytoplasmic and nuclear compartments, was obtained. The average nuclear AEC OD was then calculated for each individual case.

Survival analysis. Yu (GSE6919) and Glinsky (http://www.ordwayresearch.org/Glinsky-Supplemental2.html) cohorts were used to check the association between EZH2 directly regulated genes and clinical outcomes of patients by Kaplan–Meier analysis. The Yu cohort has 61 primary prostate cancer patients and the Glinsky cohort has 80. Significant association with outcome was determined by log-rank test for survival. Hazard ratios were calculated by the Cox proportional model. All statistics were analyzed with the statistical software R (version 2.12.1), available from the R Project for Statistical Computing website (http://www.r-project.org). We split patients into two groups by ranking the sum of EZH2-activated/repressed genes expression level in clinical cohort. The mean gene expression level across patients is centered to zero for each gene to remove the basal expression level differences. *P*-values were calculated using logrank test. In order to generate a comparable control to show that the predictive significance of clinical outcomes using EZH2-regulated genes is not by chance, we simulated 10,000 randomizations by randomly selecting the same number of genes from a cohort to predict clinical outcomes using the same model, and found the probability that a random set of genes would yield an equally significant prediction of clinical outcomes in these cohorts is 0.36% (Fig. 2D) and 1.7% (fig. S8C), respectively.

Supplementary Figure Legends

Supplementary Figure 1. Confirmation of EZH2 knockdown by the specific shRNAs. LNCaP and abl cells were transduced with lentiviral shRNAs targeting either scrambled control (shCtrl) or EZH2 (shEZH2#1 and #4), and subjected to puromycin selection (2-4 μg/ml). The whole cell lysates from LNCaP and abl stable clones were collected and subjected to immunoblotting with indicated antibodies.

Supplementary Figure 2. Confirmation of EZH2 gene activation in hormone-refractory prostate cancer cell lines (*35, 36*)**. A.** LNCaP and abl cells were transfected with either control siRNA (siCtrl) or two independent siRNAs targeting EZH2 (siEZH2#1 and #2). 48 hrs after transfection, total RNA was isolated and real-time RT-PCR was performed. mRNA levels were presented as means ± SD from three independent replicates relative to *GAPDH* level as the internal control. Insert, immunoblot of the whole cell lysates from LNCaP and abl cells 72 hrs after transfection with indicated antibodies. **B.** LNCaP, C4-2B and CWR22Rv1 cells were transfected with either control siRNA (siCtrl) or siRNA targeting EZH2 (siEZH2). 48 hrs after transfection, total RNA was isolated and real-time RT-PCR was performed. mRNA levels were presented means ± SD relative to *GAPDH* level as the internal control.

Supplementary Figure 3. Clinical relevance of EZH2-regulated genes in the Yu cohort (*8*)**. A.** Heat map of zero-centered (basal expression level removed) gene expression levels in the Yu cohort for EZH2-repressed genes in LNCaP (left panel) and EZH2-activated genes in abl (right panel). Top color bars indicate the sample types: normal (green), primary tumor (PCA, yellow) and castration-resistant prostate cancer (CRPC, orange). The color scale indicates the zero-centered expression index (normalized by RMA). **B.** Box plots of Pearson correlation coefficients (PCC) between EZH2 and EZH2-repressed genes in LNCaP (left panel) or EZH2-stimulated genes in abl (right panel). Color codes indicate the same tissue sample types as defined in **A**. *P*-values were calculated using Wilcoxon signed-rank test.

Supplementary Figure 4. Confirmation of EZH2 binding to a series of ensemble and solo peaks. A. Direct ChIP of EZH2 recruitment to either ensemble or solo binding sites was performed in abl cells using indicated antibodies. **B.** Abl cells were transfected with either control siRNA (siCtrl) or two independent siRNAs targeting EZH2 (siEZH2#1 and #2). 72 hrs after transfection, direct ChIP was performed using primers flanking a series of ensemble and solo peaks as indicated.

Supplementary Figure 5. Summary of EZH2 ensemble or solo peaks. A. Genome-wide distribution of the defined EZH2 ensemble or solo peaks in LNCaP and abl cells relative to known genes using *cis*-regulatory element annotation system (CEAS) (*37*). **B.** The size of EZH2 peak is standardized to ±1 kb around EZH2 peak summit. Peaks that overlap are merged together. The final overlaps between LNCaP and abl cells were done on the merged regions for ensemble (left panel) or solo (right panel) peaks. **C.** Venn diagrams show the overlaps of genes with EZH2 ensemble (left panel) or solo peaks (right panel) at the promoter (±5 kb around transcription start sites) or gene body regions between LNCaP and abl cells. Percentages, the overlapped number of peaks (**B**) or genes (**C**) as the percentage of the total numbers in abl.

Supplementary Figure 6. Summary of EZH2-regulated genes in abl cells. A. Numbers of genes down-regulated (black bar) and up-regulated (gray bar) upon EZH2 silencing. $P<0.05$. **B.**

Numbers of EZH2-stimulated genes that contain either EZH2 solo peaks (black bar) or H3K27me3 peaks (gray bar) within 20 kb from the transcription start sites.

Supplementary Figure 7. Regulation of EZH2 on the levels of histone marks at solo or ensemble peaks. A. Abl cells were transfected with control siRNA (siCtrl) or siRNAs against EZH2 (siEZH2). 72 hrs after transfection, direct ChIP was performed using specific antibodies targeting H3K4me2, H3K4me3 or H3K27me3, followed by quantitative PCR (qPCR) with primers flanking selected solo or ensemble sites. Data was presented as the box plots of the minimum to maximum ratios between qPCR values of siEZH2 over those of siCtrl at selected sites. **B.** Scatter plots of the minimum to maximum ratios between qPCR values of siEZH2 over those of siCtrl for H3K4me2 and H3K4me3 signals at solo peaks classified as groups near transcription start sites (TSS) or enhancer regions (enhancers).

Supplementary Figures 8. Clinical relevance of EZH2 directly regulated genes identified in prostate cancer cells. A. Oncomine concept map analysis of EZH2-activated genes that contain solo sites within 20 kb from the transcription start sites in abl (*38*). Each circle indicates a gene signature from public prostate cancer cohorts. Each line indicates the overlap significance between two linked signatures. The size of the circle is proportional to the number of genes in the signature. The width of the line is proportional to the logarithm transformed significant level [-log2 (q value)] of the overlap. The network is plotted using software gephi (http://gephi.org/). **B.** Kaplan Meier plots of EZH2 directly repressed genes in LNCaP using the Yu cohort (*8*). **C.** Kaplan Meier plots of EZH2 directly activated genes in abl (left panel) or EZH2 directly repressed genes in LNCaP (right panel) using the Glinsky cohort (*10*). **D.** Kaplan Meier plots of specific lists of genes as indicated using the Yu cohort (*8*). The numbers in the brackets indicate the number of genes in each group that are also available in the cohort. The patients are ranked by the sum of zero-centered, RMA-normalized expression levels of all genes in each group. Red (blue) curve is the survival curve for the top (bottom) 45% patients with highest (lowest) overall gene expression level. *P*-values were calculated using logrank test. *n*, numbers of the patients.

Supplementary Figure 9. Regulation of other PRC2 core subunits on EZH2 transactivation function. A. The Pearson correlation of logarithm transformed average binding signals of EZH2, H3K27me3 and SUZ12 in the union of their enriched regions. The size of each enriched region is standardized to ±1 kb around peak summit. **B.** Abl cells were transfected with either control siRNA (siCtrl) or siRNA targeting SUZ12 (siSUZ12). 72 hrs after transfection, cells were collected and subjected to direct ChIP against EZH2 followed by qPCR. Primers flanking KIAA0066 promoter regions were used as a negative control (*39*). Inserts, immunoblot of the whole cell lysates from abl cells using indicated antibodies. **C.** LNCaP and abl cells were transfected with control siRNA (siCtrl) or siRNA targeting SUZ12 (siSUZ12) or EED (siEED). 48 hrs after transfection, total RNA was isolated and amplified by real-time RT-PCR using gene specific primers as indicated. mRNA levels are presented as means ± SD relatively to *GAPDH* level as the internal control.

Supplementary Figure 10. Requirement of EZH2 catalytical activity for the androgen-independent growth and gene activation. A. Abl cells were co-transfected with siRNA against EZH2 (siEZ#4) and empty vector (siCtrl) or plasmids expressing wild-type EZH2 (E^{sr}-WT), H694A/F672I double-point mutation (E^{sr}-DM) or SET domain deletion (E^{sr}-ΔSET), all of which are Myc-tagged and siEZ#4-resistant. 72 hrs after transfection, nuclear extracts were collected and subjected to immunoblotting with indicated antibodies. **B.** Replacement experiments were

performed in CWR22Rv1 as indicated. Cells were kept in hormone-depleted medium, and collected at indicated days for direct cell counting. Data represent means ± SD. *P*-values were calculated using unpaired Student's *t*-test. **C.** Replacement experiment was performed in LNCaP as indicated. Both LNCaP and abl cells were kept in hormone-depleted medium for 72-96 hrs before nuclear extracts were prepared and subjected to immunoblotting with indicated antibodies.

Supplementary Figure 11. Enrichment of AR chromatin binding signals around the center of EZH2 solo peaks. A. The histogram of the distance of AR motif hits from EZH2 solo peak summit in abl cells. CisGenome is used for motif scan with default parameters to generate the position of AR motif hits (*40*). The enrichment of AR relative to EZH2 solo summit is calculated using BINOCh (*41*). **B.** Heat maps of AR and EZH2 solo (left panel) or ensemble (right panel) binding signal ±1 kb around EZH2 peak summit in abl cells. The color scale indicates average binding signal at 10bp window resolution. Numbers along the left sides of the columns are the index of EZH2 peaks.

Supplementary Figure 12. The functional domains of EZH2 that are involved in the physical interaction with AR. A. Top, schematic description of EZH2 deletion mutants; bottom, abl cells were infected with lentiviral shRNA against EZH2 (shEZH2), which targets against the 3' UTR of *EZH2* gene, and co-transfected with the indicated plasmids expressing either wild-type EZH2 or the various EZH2 truncation mutants, all of which are FLAG-tagged. 72 hrs after transfection, nuclear extracts were prepared and incubated with FLAG-M2 beads, followed by immunoblotting with indicated antibodies. **B.** Abl cells were infected with lentiviral shRNA against EZH2 (shEZH2) as described above and co-transfected with constructs expressing either wild-type EZH2 (EZH2-WT) or the SET domain deletion (EZH2ΔSET). 72 hrs after infection, whole cell lysates were prepared and immunoprecipitation was performed using EZH2 antibody, followed by immunoblotting with indicated antibodies.

Supplementary Figure 13. Comparison of the cistromes and transcriptomes of AR and EZH2. A. The number of base pairs overlapped between AR and EZH2 binding regions in LNCaP and abl cells. AR cistromes are derived from previous publication (*24*). Data was presented as the ratio between observed overlap and random overlap. **B.** The Venn diagrams of overlapping between AR- and EZH2-dependent genes in LNCaP and abl cells. $P<0.05$, fold change>1.5. Hypergeometric distribution is used to calculate the *p* values in both panels.

Supplementary Figure 14. Regulation of AR by EZH2 at transcriptional level or post-translational level. A. LNCaP and abl cells were transfected with control siRNA (siCtrl), or siRNAs targeting AR (top panel, siAR) or EZH2 (bottom panel, siEZH2). Biological triplicates were included for the gene expression microarray analyses. The expression raw data for AR-dependent genes were derived from our previous work (*24*). The color scale indicates the zero-centered expression index processed by RMA. **B.** Abl cells were co-transfected with siRNA against EZH2 (siEZ#4) and empty vector (Control) or plasmids as indicated. 72 hrs after transfection, nuclear extracts were prepared and immunoprecipitated with pan-methyl-Lysine or control IgG antibodies, followed by immunoblotting with indicated antibodies.

Supplementary Figure 15. Cooperative effects of AR and EZH2 on their chromatin binding and the expression of their co-activated genes. A and C. Abl cells were transfected with either control siRNA (siCtrl) or siRNA targeting EZH2 (**A**) or AR (**C**). 72 hrs after transfection, direct

ChIP against AR or EZH2 was performed followed by qPCR. The DAB2IP promoter (**A**) and the PSA enhancer (**C**) served as positive controls (*3, 33*); the KIAA0066 promoter was used as negative control (*39, 42*). **B.** Abl cells were transfected with either control siRNA (siCtrl) or siRNAs targeting EZH2 (siEZH2). 72 hrs after transfection, direct ChIP against AR was performed, followed by qPCR using primers flanking chromatin sites bound by AR only or sites overlapped by AR and EZH2 ensemble peaks. Data was presented as the box plots of the minimum to maximum values of qPCR results at selected sites. **D.** Abl cells were transfected with control siRNA, siRNAs targeting AR (siAR), EZH2 (siEZH2) or both. 48 hrs after transfection, total RNA was isolated and analyzed by real-time RT-PCR. mRNA levels are presented as means ± SD relatively to *GAPDH* levels as the internal control. Insert, immunoblot of the whole cell lysates from abl cells with indicated antibodies.

Supplementary Figure 16. Requirement of EZH2 phosphorylation at S21 for its gene activation function as well as its recruitment to solo sites. A. LNCaP (for *DAB2IP* expression) and abl (for *KIAA0101* and *RAD51C* expression) were co-transfected with siRNA against EZH2 (siEZ#4) and empty vector (siCtrl) or plasmids expressing wild-type EZH2 (E^{sr}-WT) or phosphorylation residue mutants (E^{sr}-S21A, E^{sr}-T350A and E^{sr}-T492A), all of which are Myc-tagged and siEZ#4-resistant. 48-72 hrs after transfection, cells were collected and analyzed by real-time RT-PCR. mRNA levels are presented as means ± SD relatively to *GAPDH* levels as the internal control. Insert, immunoblot of the whole cell lysates from abl cells using indicated antibodies. **B.** Direct ChIP was performed in abl cells using specific antibodies against IgG (IgG), phsophorylated EZH2 at S21 (pS21), at T350 (pT350) or at T492 (pT492). qPCR was followed using primers flanking indicated sites.

Supplementary Figure 17. Requirement of EZH2 phosphorylation at S21 for the androgen-independent growth of prostate cancer cell lines. A-C. Replacement experiments were performed in CWR22Rv1 (**A**), C4-2B (**B**) and LNCaP (**C**) cells as indicated. Cells were maintained in androgen-depleted medium, and collected at indicated days for direct counting. Data represent means ± SD. *P*-values were calculated using unpaired Student's *t*-test.

Supplementary Figure 18. Up-regulation of AKT-mediated phosphorylation of EZH2 at S21 in CRPC cells. A. Nuclear extracts were prepared from LNCaP, CWR22Rv1 and C4-2B cells, and subjected to immunoblotting with indicated antibodies. **B.** LNCaP and abl cells were treated without (-) or with (+) 10 nM DHT for 24 hrs. The whole cell lysates were prepared and subjected to immunoblotting with indicated antibodies.

Supplementary Figure 19. The protein levels of EZH2, phosphorylated EZH2 at S21 [pEZH2(S21)] and H3K27me3 in prostate tumors. A-C. Immunohistochemistry (IHC) staining of EZH2 (**A**), pEZH2(S21) (**B**), and H3K27me3 (**C**) in neoadjuvant primary prostate tumors. **D-F.** IHC of EZH2 (**D**), pEZH2(S21) (**E**), and H3K27me3 (**F**) in CRPC.

Supplementary Figure 20. Model of EZH2 functional switch from a Polycomb repressor to a transcriptional activator in CRPC. PI3K/AKT pathway activation, through PTEN loss and/or down-regulation of the phosphatase PHLPP1, leads to phosphorylation of EZH2 at S21. This phosphorylation event shifts EZH2 from a transcriptional repressor associated with PRC2 to a transcriptional co-activator cooperating with AR, which an intact SET methyltransferase domain. Our work suggests that EZH2 along with AR and the PI3K/AKT pathway are potential therapeutic targets in CRPC (highlighted in green).

Supplementary Figure 1

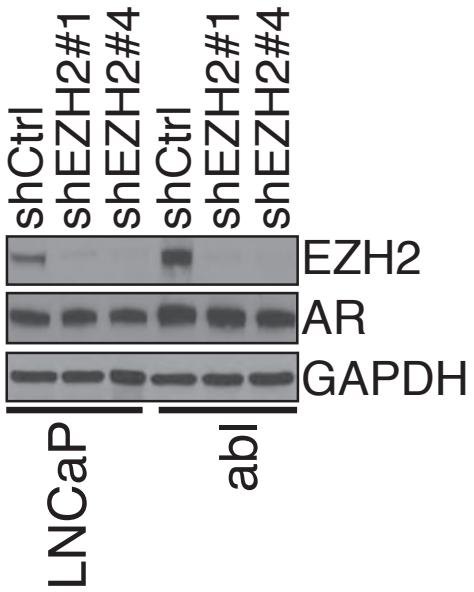

Supplementary Figure 2

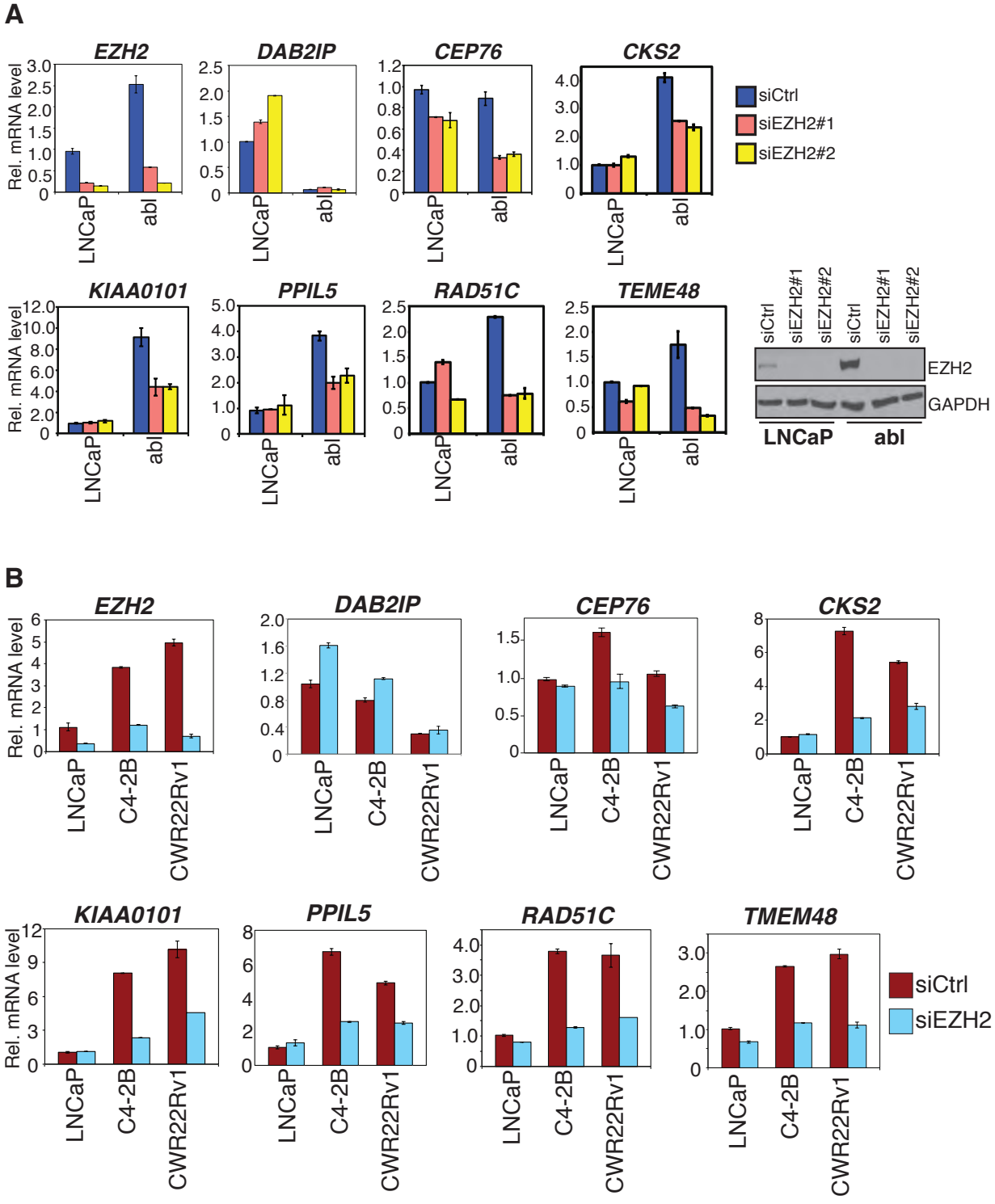

Supplementary Figure 3

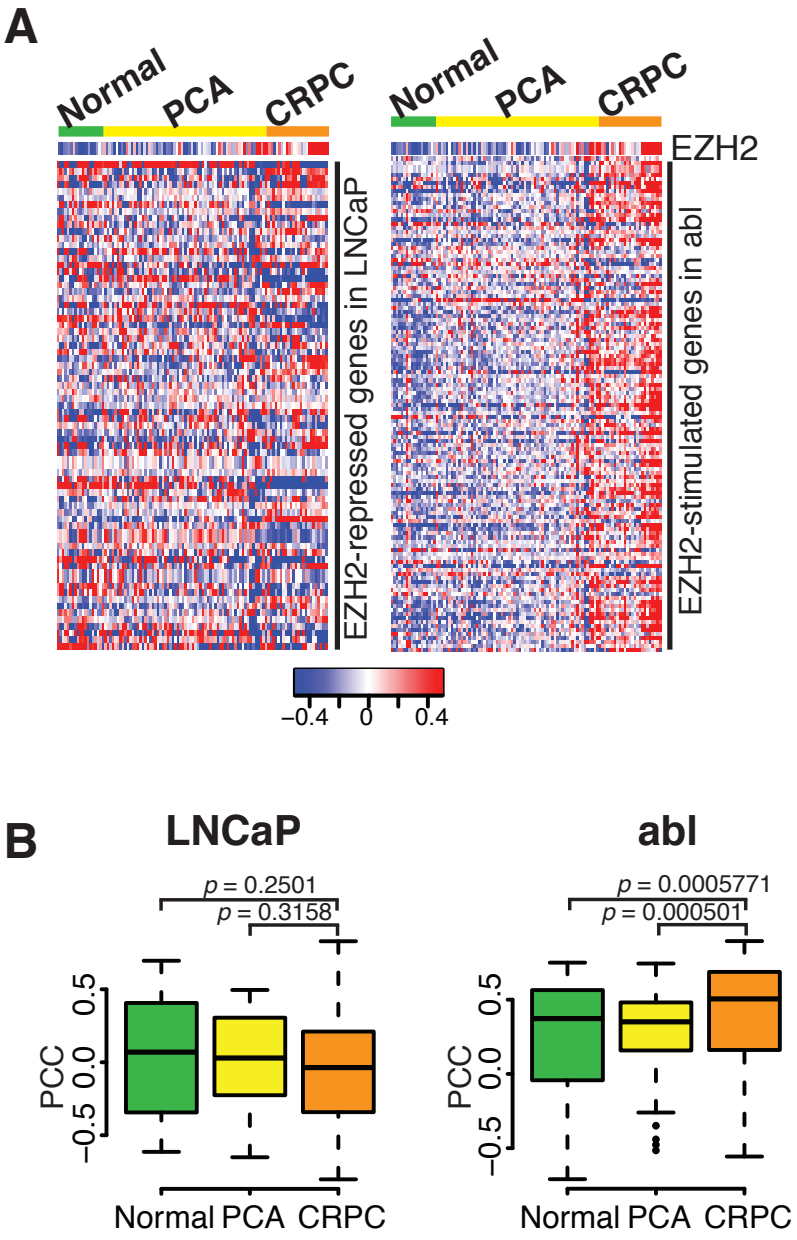

Supplementary Figure 4

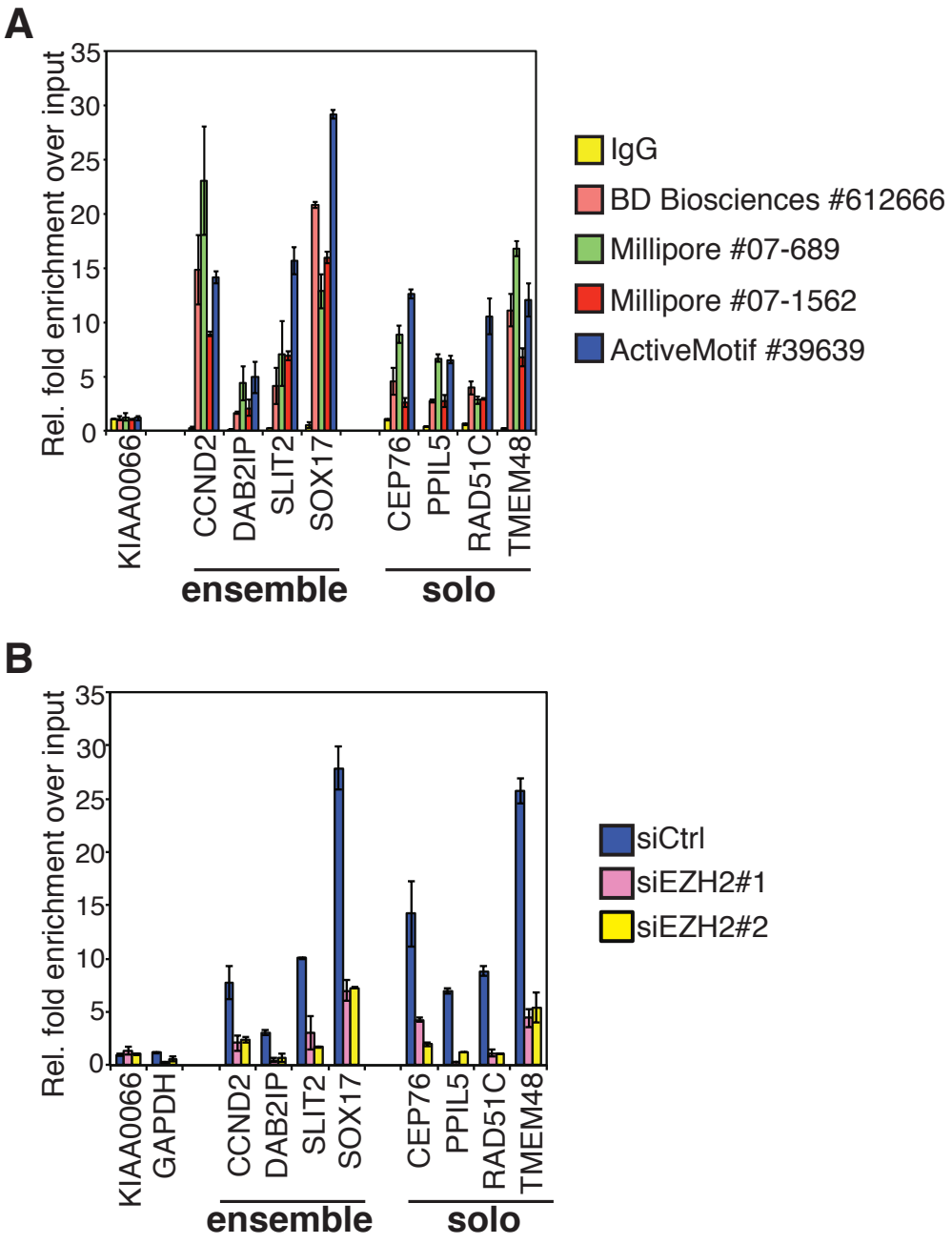

Supplementary Figure 5

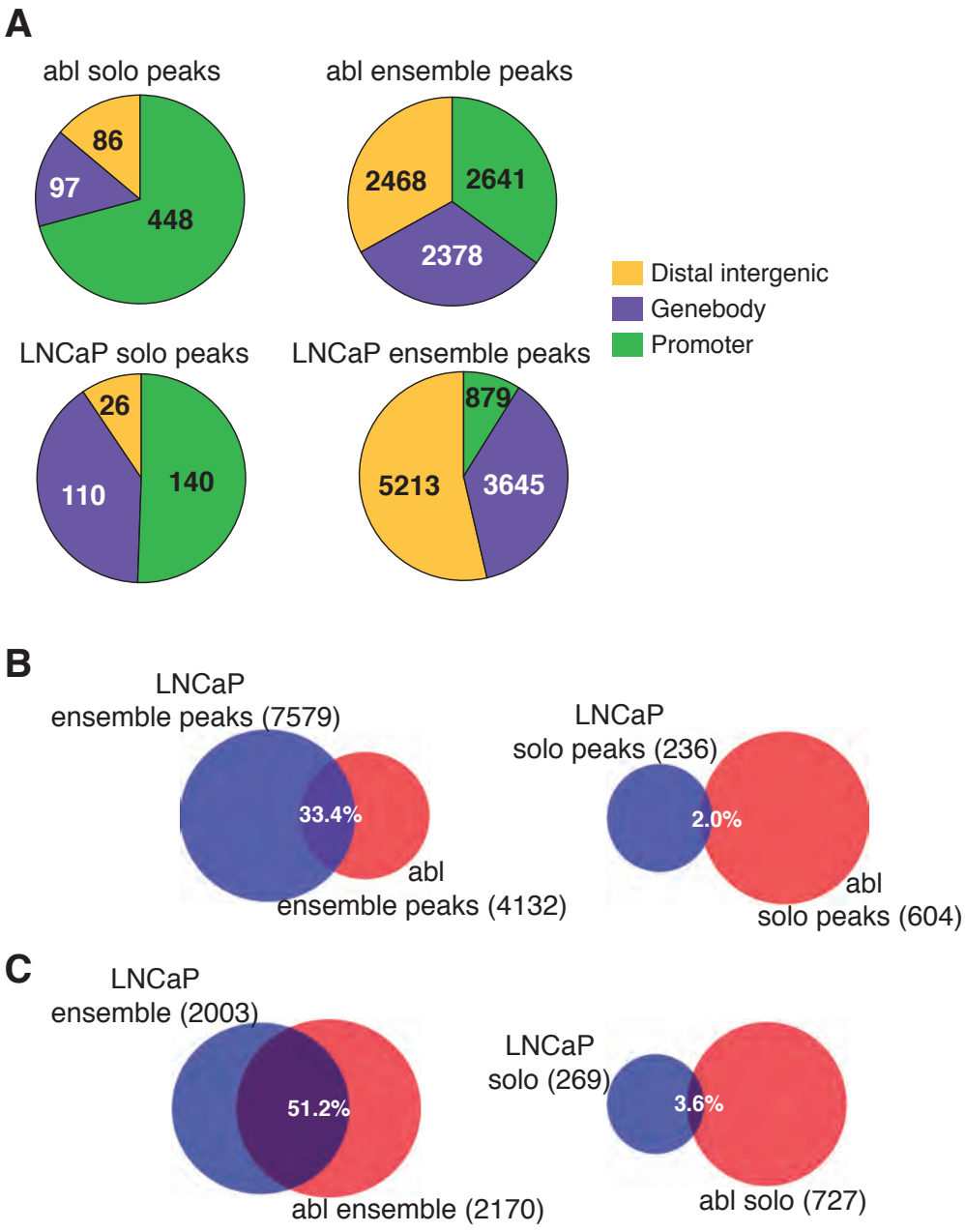

Supplementary Figure 6

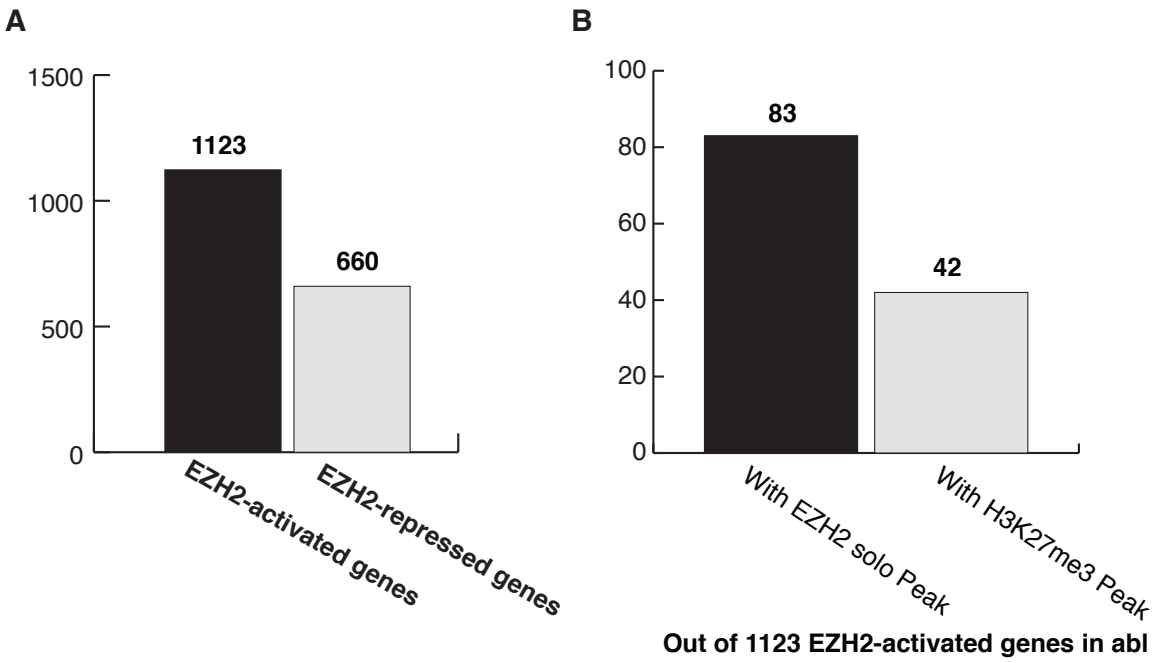

Supplementary Figure 7

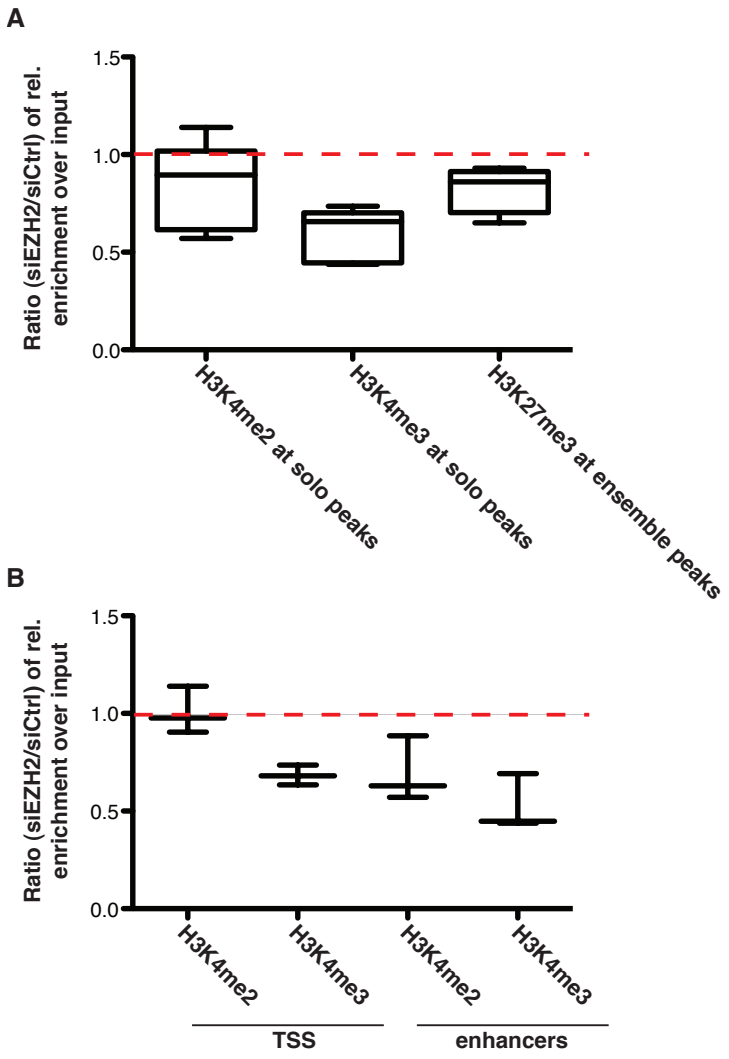

Supplementary Figure 8

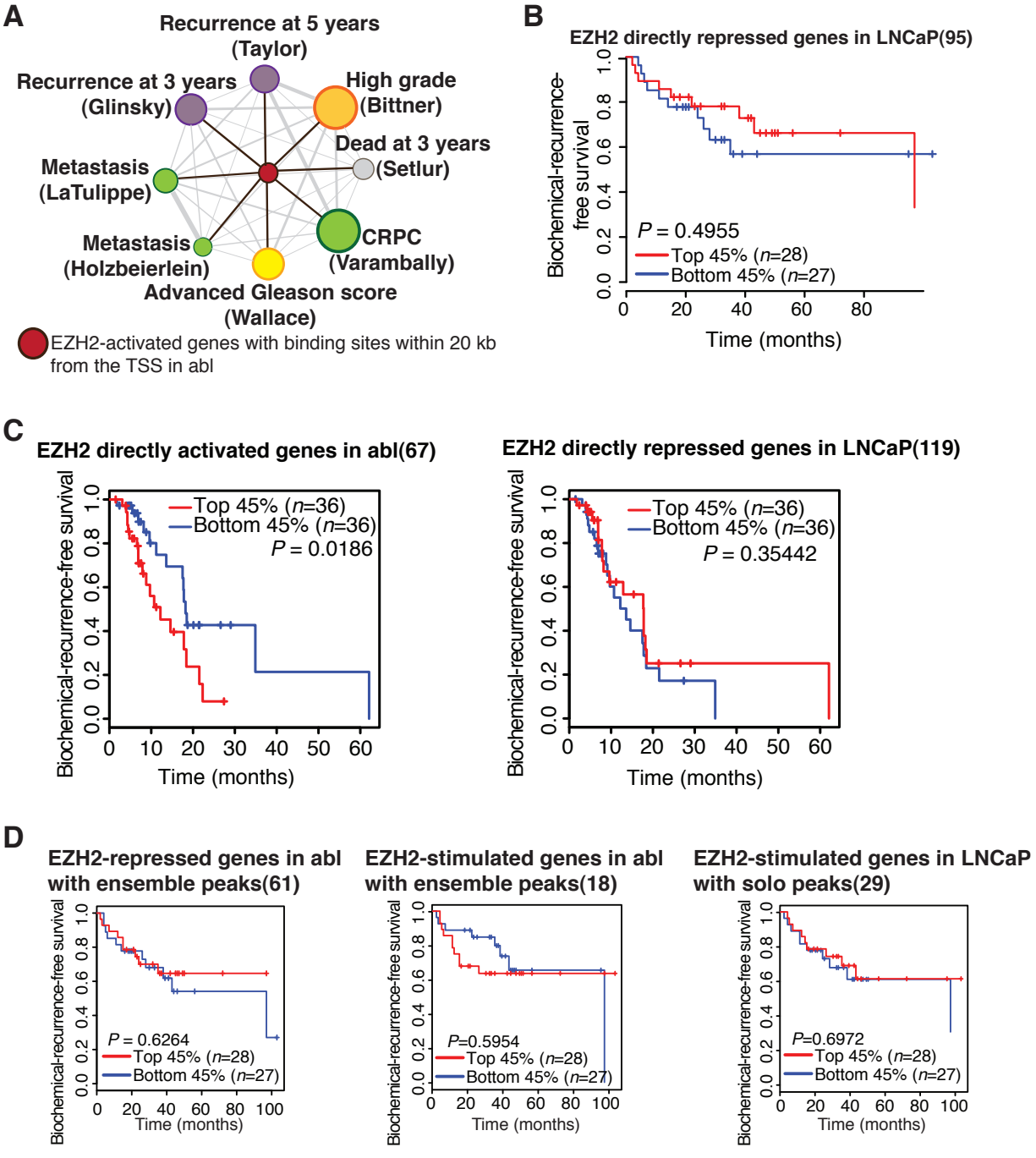

Supplementary Figure 9

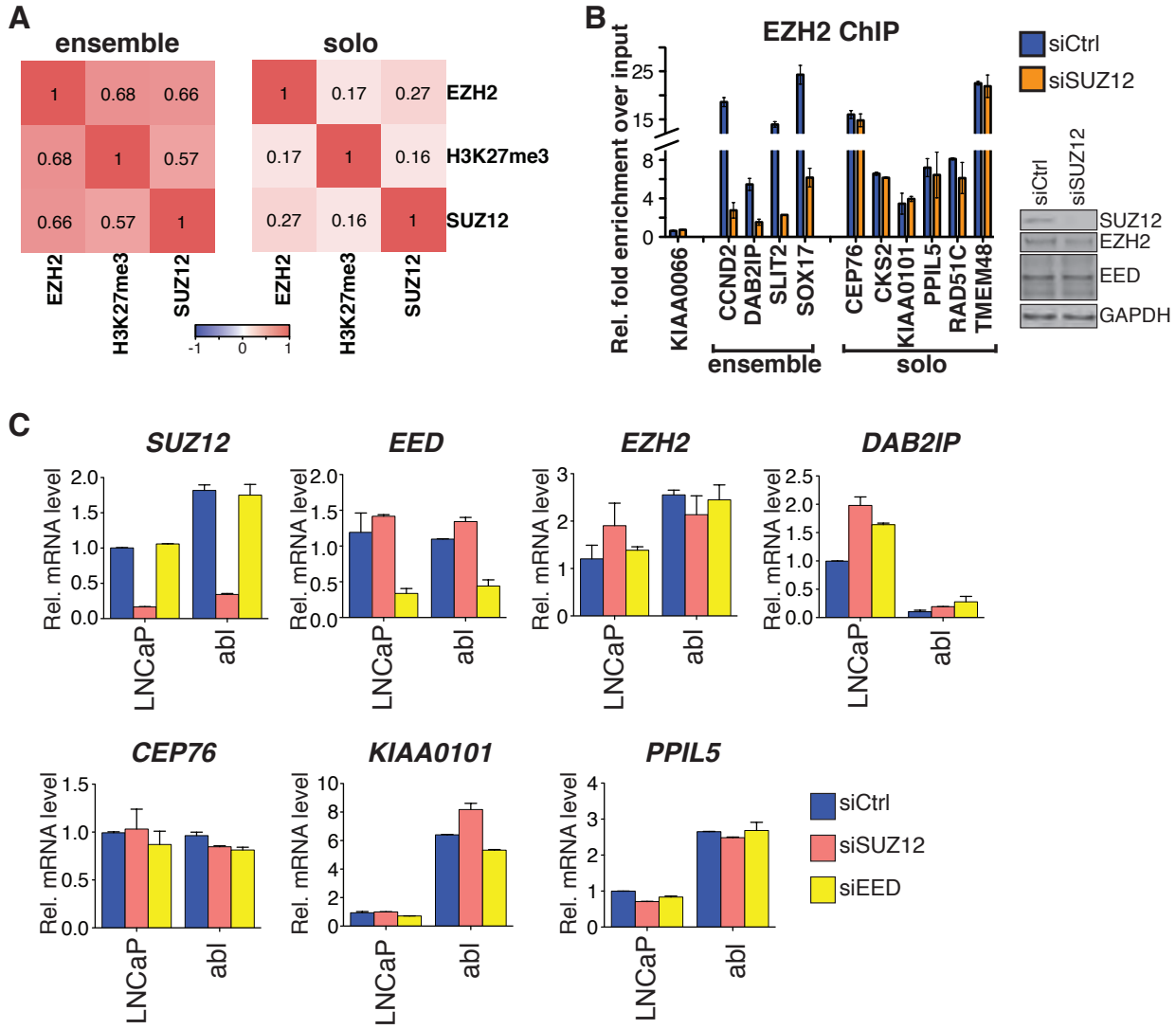

Supplementary Figure 10

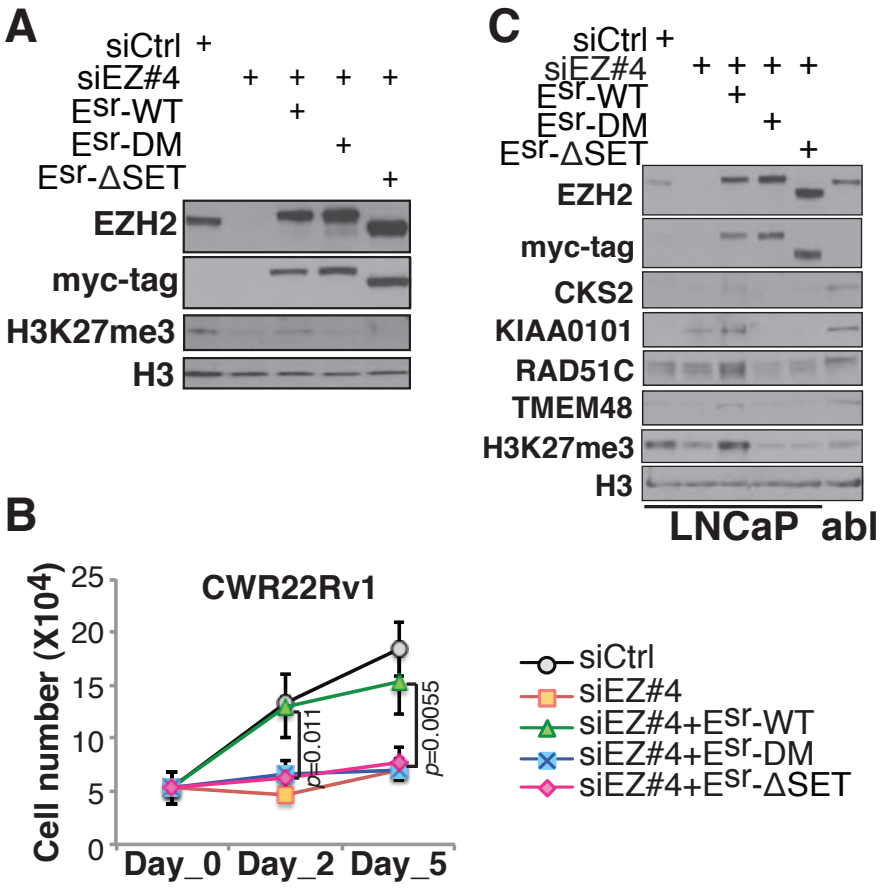

Supplementary Figure 11

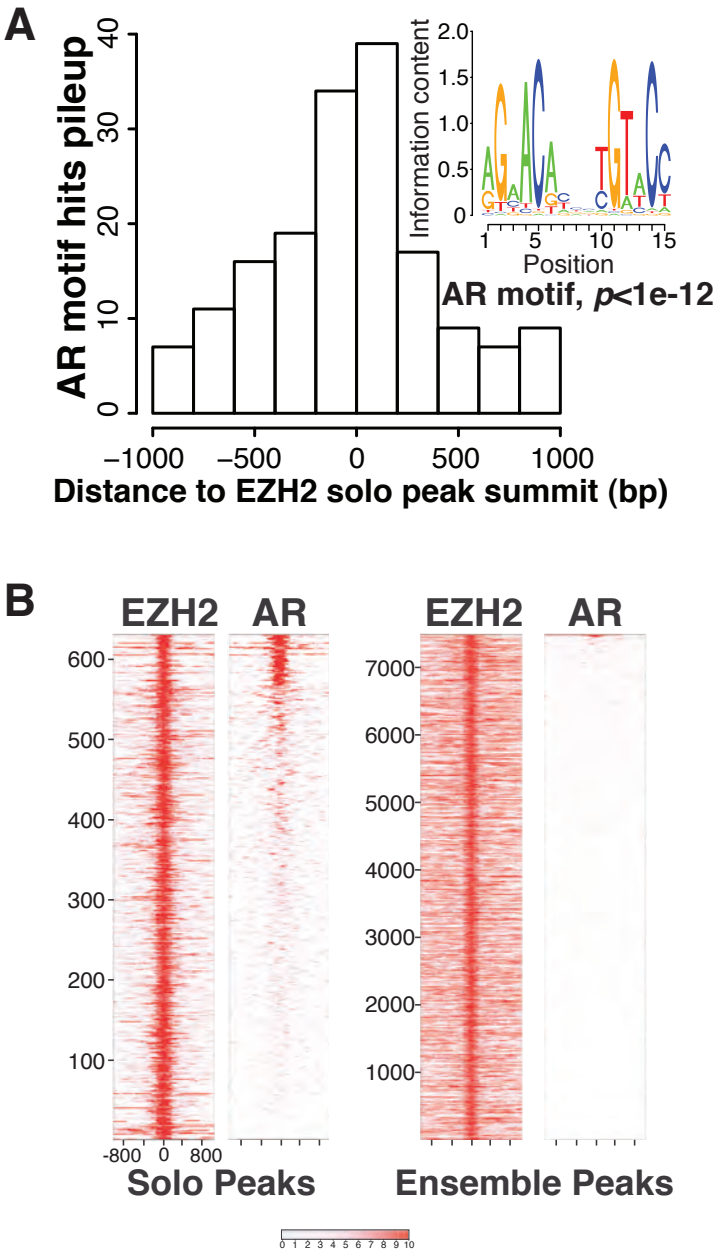

Supplementary Figure 12

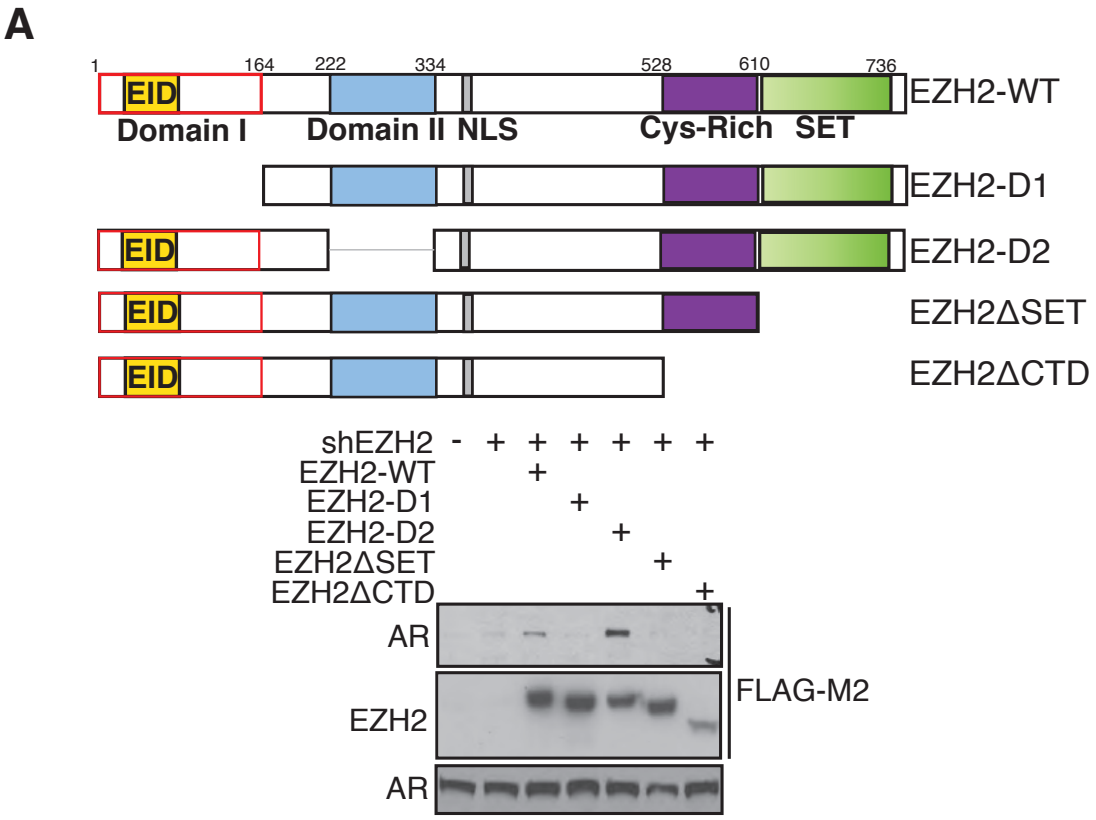

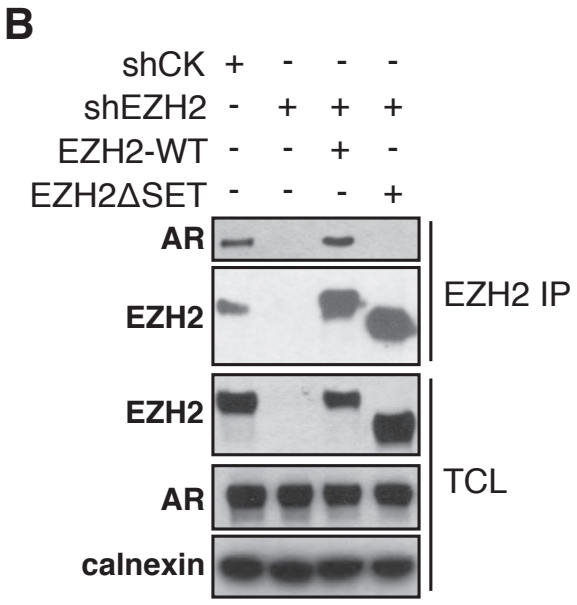

Supplementary Figure 13

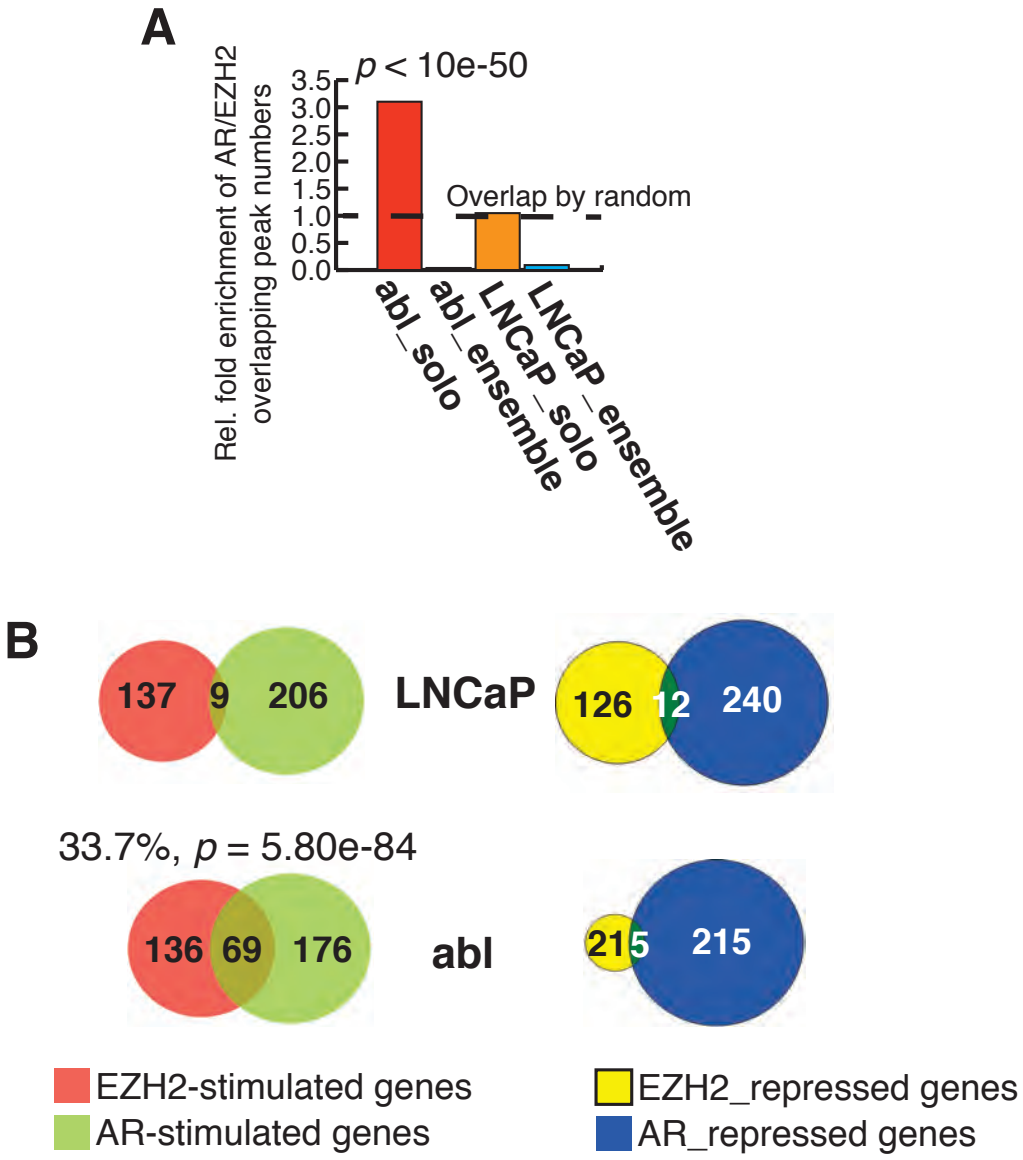

Supplementary Figure 14

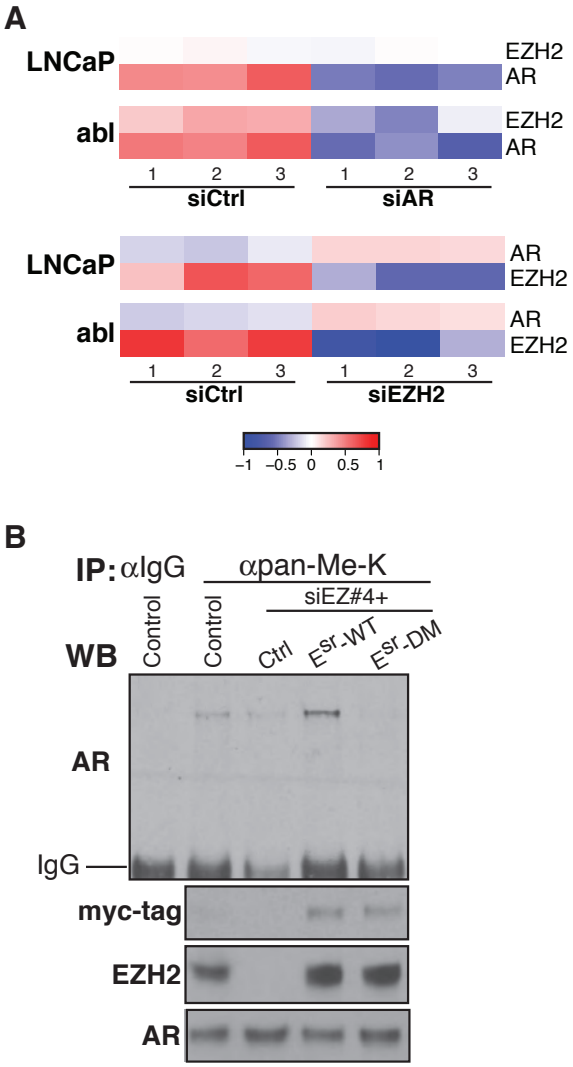

Supplementary Figure 15

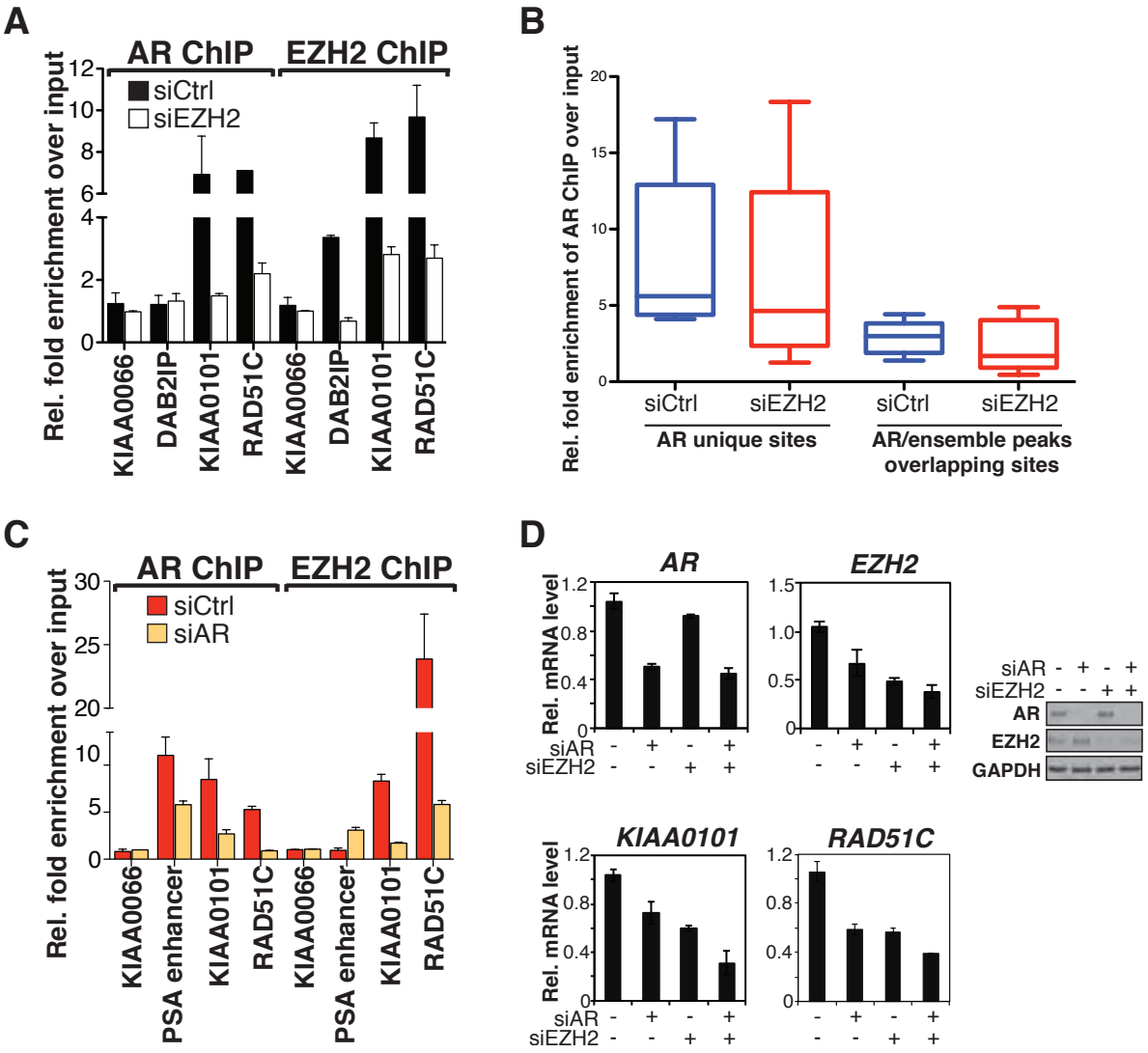

Supplementary Figure 16

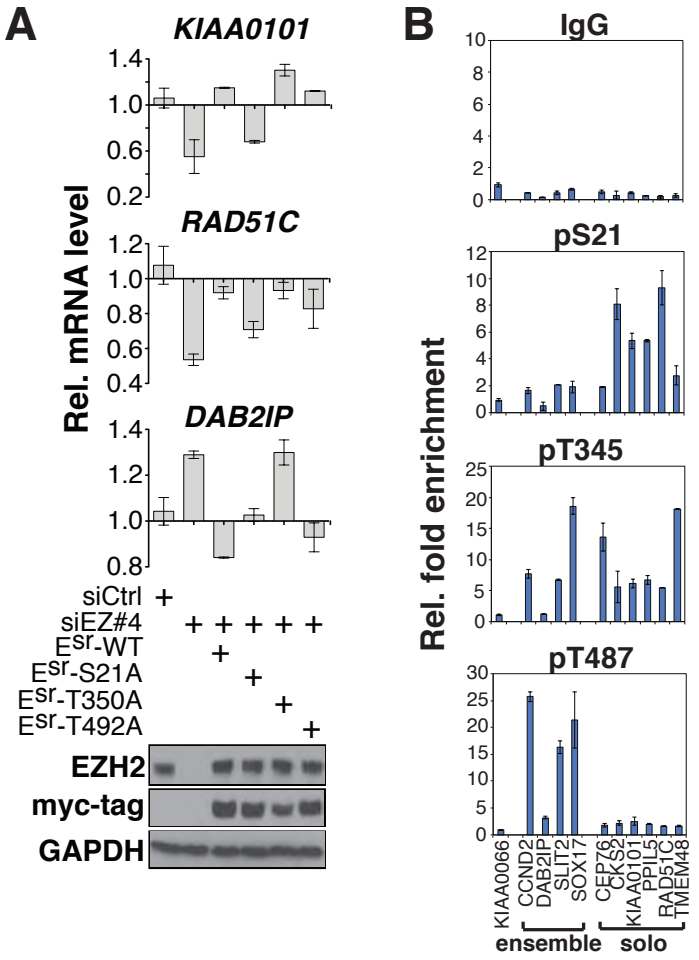

Supplementary Figure 17

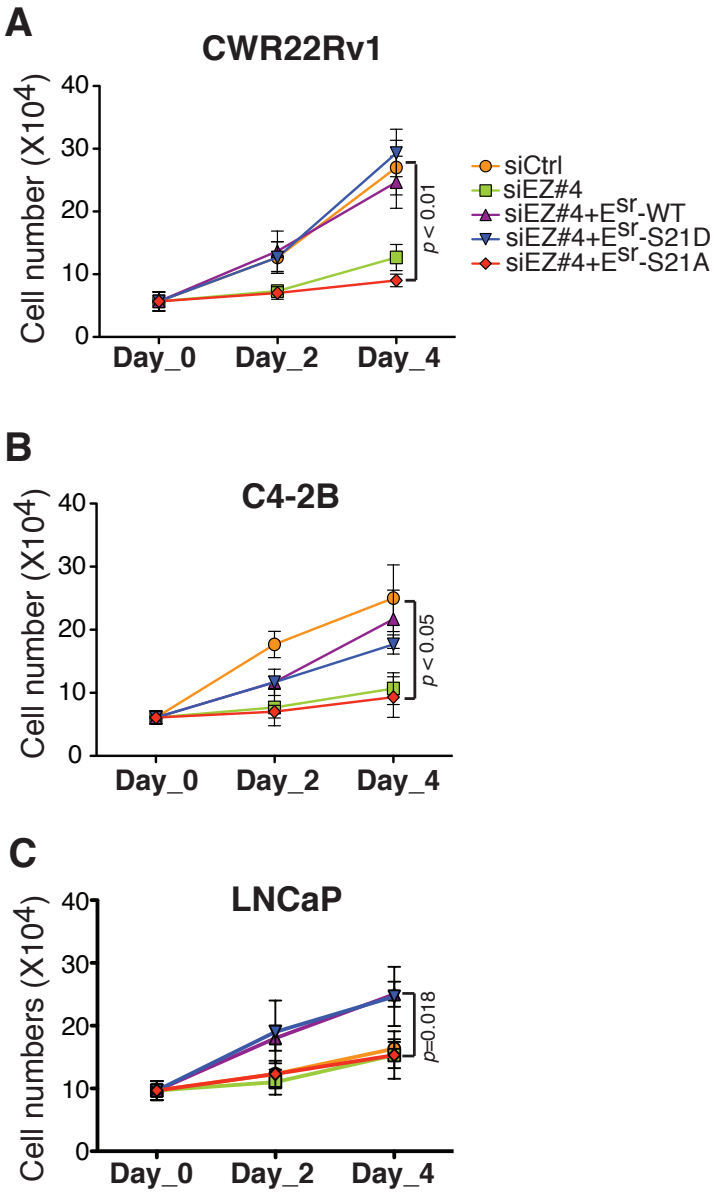

Supplementary Figure 18

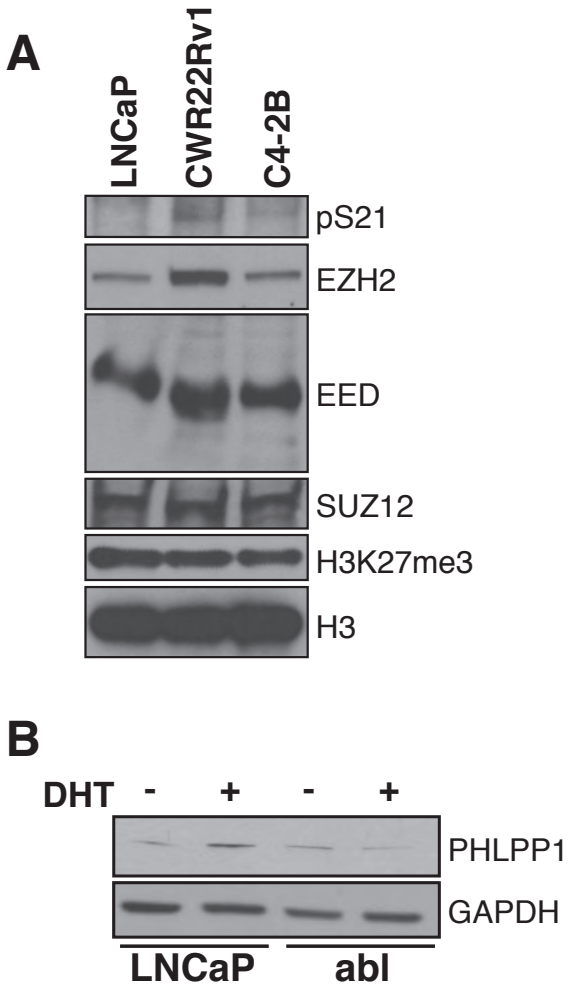

Supplementary Figure 19

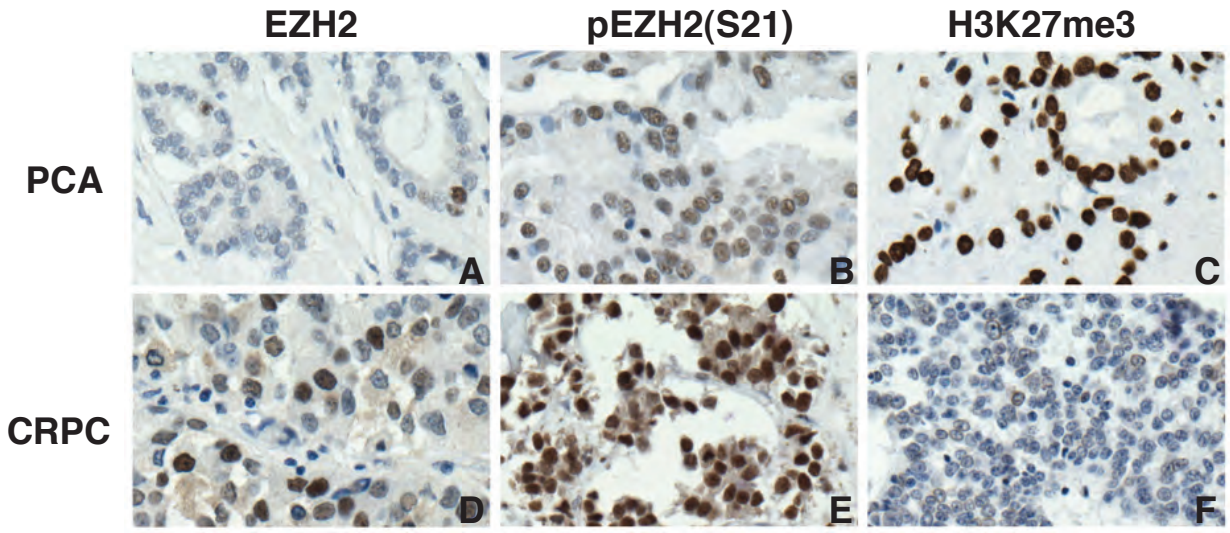

Supplementary Figure 20

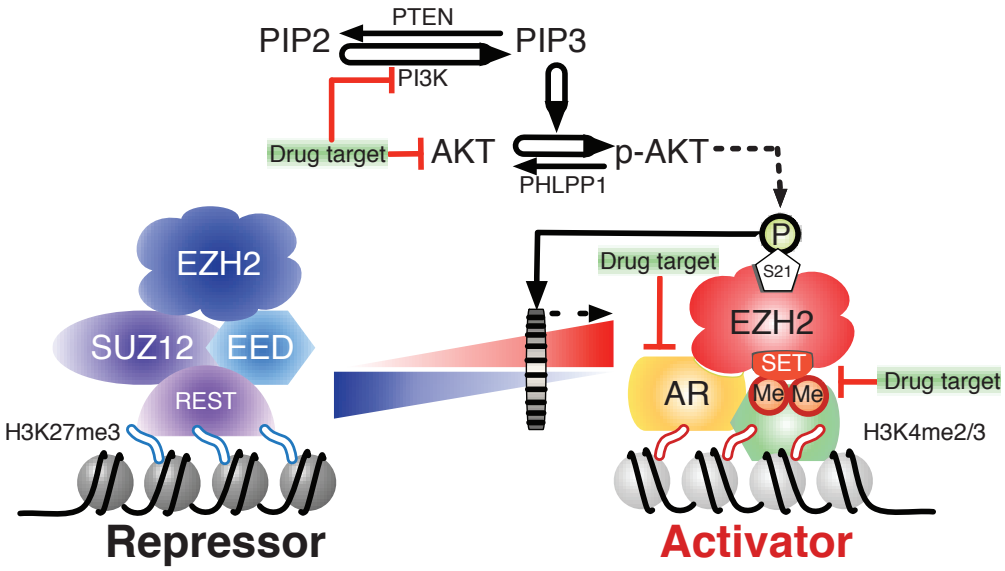

Supplementary Table 1: EZH2-stimulated genes bound by EZH2 solo peaks in abl cells

PA2G4	proliferation-associated 2G4, 38kDa
RECQL4	RecQ protein-like 4
PKM2	pyruvate kinase, muscle
MRPL2	mitochondrial ribosomal protein L2
MRPL20	mitochondrial ribosomal protein L20
RAD23A	RAD23 homolog A (S. cerevisiae)
CHMP4A	chromatin modifying protein 4A
CCDC34	coiled-coil domain containing 34
PSMD1	proteasome (prosome, macropain) 26S subunit, non-ATPase, 1
DAND5	DAN domain family, member 5
SUDS3	suppressor of defective silencing 3 homolog (S. cerevisiae)
FKBP5	FK506 binding protein 5
USP1	ubiquitin specific peptidase 1
RAD1	RAD1 homolog (S. pombe)
VDAC2	voltage-dependent anion channel 2
TRIM28	tripartite motif containing 28
MAPKAPK5	mitogen-activated protein kinase-activated protein kinase 5
ATAD2	ATPase family, AAA domain containing 2
KIAA0101	KIAA0101
KIF2C	kinesin family member 2C
CAD	carbamoyl-phosphate synthetase 2, aspartate transcarbamylase, and dihydroorotase
NFYB	nuclear transcription factor Y, beta
BRIX1	BRX1, biogenesis of ribosomes, homolog (S. cerevisiae)
LRR1	leucine rich repeat protein 1
SRSF1	serine/arginine-rich splicing factor 1
ADK	adenosine kinase
HAGH	hydroxyacylglutathione hydrolase
SMC2	structural maintenance of chromosomes 2
CDT1	chromatin licensing and DNA replication factor 1
GPR137	G protein-coupled receptor 137
DDX55	DEAD (Asp-Glu-Ala-Asp) box polypeptide 55
TOR3A	torsin family 3, member A
SYCE2	synaptonemal complex central element protein 2
TIMM13	translocase of inner mitochondrial membrane 13 homolog (yeast)
GADD45GIP1	growth arrest and DNA-damage-inducible, gamma interacting protein 1
PSMG3	proteasome (prosome, macropain) assembly chaperone 3
IQGAP3	IQ motif containing GTPase activating protein 3
CHEK1	CHK1 checkpoint homolog (S. pombe)
MRPL11	mitochondrial ribosomal protein L11
CENPK	centromere protein K
RNPS1	RNA binding protein S1, serine-rich domain

DAZAP1	DAZ associated protein 1
MRPS7	mitochondrial ribosomal protein S7
CKS2	CDC28 protein kinase regulatory subunit 2
TONSL	tonsoku-like, DNA repair protein
TAF12	TAF12 RNA polymerase II, TATA box binding protein (TBP)-associated factor, 20kDa
LSM2	LSM2 homolog, U6 small nuclear RNA associated (S. cerevisiae)
NUP85	nucleoporin 85kDa
MCM7	minichromosome maintenance complex component 7
PPP1R10	protein phosphatase 1, regulatory (inhibitor) subunit 10
MCM4	minichromosome maintenance complex component 4
LRRC40	leucine rich repeat containing 40
ARL6IP1	ADP-ribosylation factor-like 6 interacting protein 1
RAD51C	RAD51 homolog C (S. cerevisiae)
C21orf59	chromosome 21 open reading frame 59
C11orf83	chromosome 11 open reading frame 83
UBE2I	ubiquitin-conjugating enzyme E2I
POLR2E	polymerase (RNA) II (DNA directed) polypeptide E, 25kDa
RBM42	RNA binding motif protein 42
MRTO4	mRNA turnover 4 homolog (S. cerevisiae)
RNASEH2A	ribonuclease H2, subunit A
ZDHHC4	zinc finger, DHHC-type containing 4
E2F1	E2F transcription factor 1
EXOC5	exocyst complex component 5
SLC3A2	solute carrier family 3 (activators of dibasic and neutral amino acid transport), member 2
PNP	purine nucleoside phosphorylase
EIF4G1	eukaryotic translation initiation factor 4 gamma, 1
FBL	fibrillarin
CYC1	cytochrome c-1
PTMA	prothymosin, alpha
PSMD12	proteasome (prosome, macropain) 26S subunit, non-ATPase, 12
TTC33	tetratricopeptide repeat domain 33
PFN1	profilin 1
CEP76	centrosomal protein 76kDa
DTYMK	deoxythymidylate kinase (thymidylate kinase)
TMEM48	transmembrane protein 48
MYO19	myosin XIX
NRAS	neuroblastoma RAS viral (v-ras) oncogene homolog
C16orf53	chromosome 16 open reading frame 53
TUBGCP3	tubulin, gamma complex associated protein 3
DR1	down-regulator of transcription 1, TBP-binding (negative cofactor 2)
MIS18A	MIS18 kinetochore protein homolog A (S. pombe)
HEXIM1	hexamethylene bis-acetamide inducible 1

Supplementary Table 2: siRNA/shRNA sequences

siEZH2#1 (siGENOME SMARTpool)	CAAAGAAUCUAGCAUCAUA
	GAGGACGGCUUCCCAAUAA
	GCUGAAGCCUCAAUGUUUA
	GAAUGGAAACAGCGAAGGA (siEZ#4)
siEZH2#2 (ON-TARGETplus SMARTpool)	GAGGACGGCUUCCCAAUAA
	GCUGAAGCCUCAAUGUUUA
	UAACGGUGAUCACAGGAUA
	GCAAAUUCUCGGUGUCAAA
siSUZ12 (siGENOME SMARTpool)	GAACACCUAUCACACAUAU
	GCAACAAACUGAAGCAAGA
	GAACAGCAAAGAACAUAUA
	GAAUUUAUGUCGAAACUUC
siAR (siGENOME SMARTpool)	GGAACUCGAUCGUAUCAUU
	CGUGCAGCCUAUUGCGAGA
	UCAAGGAACUCGAUCGUAU
	GAAAUGAUUGCACUAUUGA
shEZH2#1	TATTGCCTTCTCACCAGCTGC
shEZH2#4	CGGAAATCTTAAACCAAGAAT

Supplementary Table 3: ChIP-qPCR primers

TACTAGCGGTTTTACGGGCG	GAPDH promoter F
TCGAACAGGAGGAGCAGAGAGCGA	GAPDH promoter R
CTAGGAGGGTGGAGGTAGGG	KIAA0066 promoter F (*42*)
GCCCCAAACAGGAGTAATGA	KIAA0066 promoter R (*42*)
TCCAACCGAAACTCCAAAAC	CCND2 promoter F
CTTTTCACCCTTCACGGAAA	CCND2 promoter R
CCTGCTCGAGTCTGCACTG	DAB2IP promoter F
TCGAATCTCTCCCATGGTTC	DAB2IP promoter R
CCAAGTTCATCCTTGGGAGA	SLIT2 promoter F
AAGGCAGTAGAGCCCACTCA	SLIT2 promoter R
AATCGCTAGGCCGATTTCTT	SOX17 promoter F
GAAGGGAACCCAGAGCCTTA	SOX17 promoter R
AACCCGGCAGTTAGCTGGAC	CEP76 promoter F
GAACGAGGGCAGCAAGCC	CEP76 promoter R
GTCCCCATTTTCCGCAAG	CKS2 enhancer F
GTCACAGCAAAGCGACAGAG	CKS2 enhancer R
CAACAAAGCAGGAAGAAGCA	KIAA0101 enhancer F
CTAGTTCCCTTCGCAACACC	KIAA0101 enhancer R
CTTTCCCTGTAACGCAGAGG	PPIL5 promoter F
GTTTCTGTTCGGGGAGGATT	PPIL5 promoter R
GCAGCCGAGTTTTCTCATTC	RAD51C enhancer F
GAGACGCTGTTGGTCCTGAT	RAD51C enhancer R
CTTCGTCTGGACAAGCTCAA	TMEM48 promoter F
GCCGTCGAGACTACAGTTCC	TMEM48 promoter R
GAGCCTCTTTCTCAGTTTTGCTTCC	FKBP5 enhancer F
TACTGCCCTAGAGCAATTTTGTTTTG	FKBP5 enhancer R
ACCCCTGTTGCTGTTCATCCTG	KLK2 promoter F
CCGCCCTTGCCCTGTTGG	KLK2 promoter R
AGTTGCCCATGCTTTGATCT	KLK2 enhancer F
TGAATGATGAGTGGATGATGC	KLK2 enhancer R
GACAACTTGCAAACCTGCTC	PSA enhancer F (*43*)
GATCCAGGCTTGCTTACTGT	PSA enhancer R (*43*)
GGACCAGGCTGTTGTCGAA	HS_5965
CTTTGGGAGGCCGAGTCA	HS_5965
GGAGCTGCTGCAGGAATCAG	BMP7 enhancer F
TGCAGAGATGAATGGGAAATAAAG	BMP7 enhancer R
GCAACCTGCCCACGAACT	CASZ1 promoter F
CTTGAATTTCAGGGTCCCTTGT	CASZ1 promoter R
AATAAGATTAAAAGCTCCAGGAAATCAG	ELP4 promoter F
AGCTTGAGGGATAGGCACACTT	ELP4 promoter R

Supplementary Table 4: mRNA real-time RT-PCR primers

CCTGGCTTCCGCAACTTACAC	AR mRNA F (*24*)
GGACTTGTGCATGCGGTACTCA	AR mRNA R (*24*)
ATTGTGTGCGATGGTTAGGC	EED mRNA F
CCATAGAAAACCTCATGTACC	EED mRNA R
TTGTTGGCGGAAGCGTGTAAAATC	EZH2 mRNA F
TCCCTAGTCCCGCGCAATGAGC	EZH2 mRNA R
TGGACGATGTGCTCTATGCC	DAB2IP mRNA F
GGATGGTGATGGTTTGGTAG	DAB2IP mRNA R
CGAGATCCCTCCAAAATCAA	GAPDH mRNA F
TTCACACCCATGACGAACAT	GAPDH mRNA R
AAACGAAATCGTGAGGATGG	SUZ12 mRNA F (*44*)
CCATTTCCTGCATGGCTACT	SUZ12 mRNA R (*44*)
GAGACTATACGGGAAGAATTGGC	CEP76 mRNA F
ACATCGTCAATGATTCCTCGAC	CEP76 mRNA R
TTCGACGAACACTACGAGTACC	CKS2 mRNA F
GGACACCAAGTCTCCTCCAC	CKS2 mRNA R
ATGGTGCGGACTAAAGCAGAC	KIAA0101 mRNA F
CCTCGATGAAACTGATGTCGAAT	KIAA0101 mRNA R
GGGACCCGCTATGAGCTAAG	PPIL5 mRNA F
CCTTTAACCGAACAGTGGCTTT	PPIL5 mRNA R
TTTGGTGAGTTTCCCGCTGTC	RAD51C mRNA F
CTCAGCAGTCTGGAACCCC	RAD51C mRNA R
AGGTCGCGGGACATACTGT	TMEM48 mRNA F
TGCAGATGGGTAGAAATAGCACT	TMEM48 mRNA R